Ultrafast anisotropic polarization dynamics of electronic ferroelectric $LuFe_2O_4$

H. Yu [1], Y. Fukada [2], G. Nishida [2], K. Takubo [1], T. Ishikawa [1], S. Koshihara [1], N. Ikeda [2], and Y. Okimoto [1,*]

[1] *Department of Chemistry, Tokyo Institute of Technology, 2-12-1 Meguro, Tokyo 152-8551, Japan*

[2] *Department of Physics, Okayama University, 3-1-1 Tsushimanaka, Okayama 700-8530, Japan*

(Received 27 February 2024; accepted 9 May 2024; published 3 June 2024)

Femtosecond time-resolved second-harmonic generation (SHG) measurements were performed at room temperature on a single crystal of $LuFe_2O_4$, which has recently attracted attention as an electronic ferroelectric material in which polarization occurs due to the real-space arrangement of Fe^{2+} and Fe^{3+}. We irradiated the crystal with 800-nm laser pulses, traced the subsequent SHG changes, and observed anisotropic polarization dynamics: immediately after photoexcitation, the in-plane (*ab*-plane) component of the SHG greatly reduced, while the interplane (*c* axis) SHG increased. This means that a hidden photoexcited state, in which the in-plane charge ordering is broken but the polarization along the *c*-axis direction enhanced, has been created by photoexcitation, indicating that the electronic ferroelectricity can be controlled on a femtosecond scale.

DOI: 10.1103/PhysRevMaterials.8.064402

I. INTRODUCTION

Ferroelectric materials have polarization (electric dipole moments) derived from their inversion symmetry-breaking crystal structures, whose direction can be controlled by electric fields. This makes ferroelectrics suitable for various industrial applications, such as memory devices. Therefore, the development of more energy-efficient and rapidly responsible ferroelectric materials is a critically important research topic in material science.

Recently, "electronic ferroelectrics" have garnered attention as a novel type of ferroelectric material [1–3]. Unlike traditional ferroelectrics, in which spontaneous polarization arises from ionic displacements or the ordering of molecules' orientations, electronic ferroelectrics exhibit spontaneous polarization due to the ordering of electrons, which breaks the inversion symmetry [4]. In electronic ferroelectrics, polarization can be altered by moving electrons, which are much lighter than ions, potentially allowing for the control of polarization at low electric fields [5] and at ultrafast speed. From this perspective, electronic ferroelectrics are anticipated as new materials that could surpass conventional ferroelectrics in performance and functions.

In 2005, Ikeda *et al.* proposed the iron composite oxide RFe_2O_4 (where *R* is a trivalent rare-earth ion) as an example of electronic ferroelectrics [1]. This crystal consists of layers of *R* ions and oxygen ions (*R* layer) and a double layer of Fe ions and oxygen ions (*W* layer) [6–8]. Notably, as shown in Fig. 1(a), in each *W* layer, Fe^{3+} (red circles) and Fe^{2+} (blue circles) demonstrate a threefold periodic charge order in the triangular lattice plane. Different numbers of Fe^{2+} and Fe^{3+} ions exist in the upper and lower layers of the *W* layer. Consequently, the *W* layer itself exhibits a dipole moment in the direction indicated by the arrows in Fig. 1(a), leading to spontaneous polarization throughout the crystal [1,5–9].

Another characteristic feature of this system is the issue of the correlation of the electric polarization along the *c* axis. The total electric polarization of the RFe_2O_4 crystal is formed by the sum of each polarization in *W* layers as shown in Fig. 1(a), but all the directions of the polarizations in a crystal are not aligned along the *c* axis. Fujiwara *et al.* demonstrated through temperature-dependent neutron-scattering measurements of $YbFe_2O_4$ that the spin correlation length along the *c* axis is approximately 50 nm at room temperature [10,11]. From this, the length of polarization alignment along the *c* axis in RFe_2O_4 is also expected to be similar order. Figure 1(b) is a schematic diagram illustrating the *c* axis correlation in RFe_2O_4. The gray block represents the stacks of some polar *W* layers aligned in the same direction. The thickness of these blocks along the *c* axis corresponds to the correlation length of electric polarization. Thus, in RFe_2O_4, not only the long-range threefold periodic order of Fe^{2+} and Fe^{3+} in the *W* layer but also the short-range correlations of the dipole moment of the *W* layer along the *c* axis, contribute to the macroscopic polarization of the system.

In this paper, we focus on $LuFe_2O_4$ among the RFe_2O_4 series and attempt to control its polarization state by manipulating electrons in iron cations using femtosecond laser pulses. For studying the polarization dynamics of ferroelectrics, the method of time-resolved second-harmonic generation (SHG) measurements is useful [3,12–19]. This method involves exciting the crystal with femtosecond pulses, and then measuring the SHG change with another laser pulse, which allows the polarization dynamics of the system to be traced on a femtosecond scale. This technique has been used for various ferroelectric materials to study the dynamics of ferroelectrics, control the polarization rapidly, and search for the so-called hidden state harbored in the ferroelectric materials [3,16,18].

In general, the SHG intensity (I_{SH}) is represented as $I_{SH} \propto |\boldsymbol{P}^{(2)}|^2 \propto |\varepsilon_0 \chi^{(2)} : \boldsymbol{EE}|^2$, using the second-order nonlinear susceptibility tensor $\chi^{(2)}$. Here, ε_0 is the permittivity in vacuum, $\boldsymbol{E}$ is the electric field of the incident light, and

*okimoto.y.aa@m.titech.ac.jp

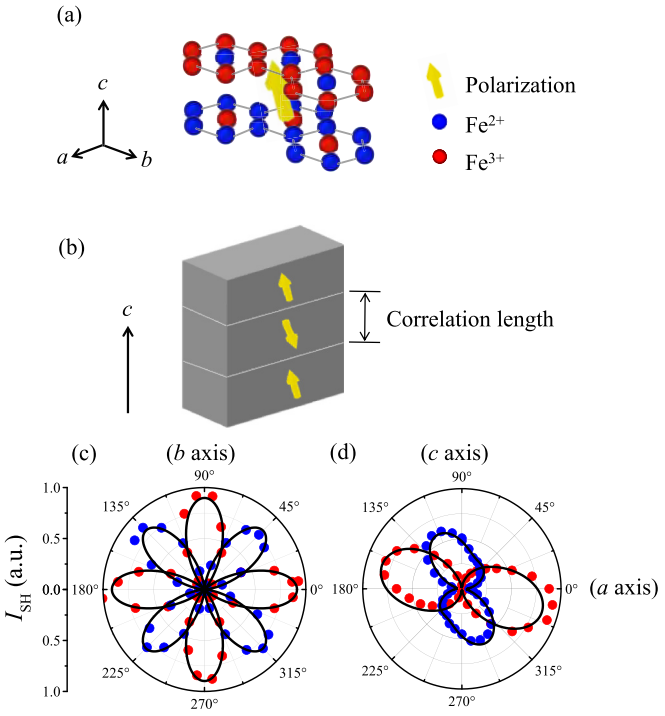

FIG. 1. (a) Schematic diagram of the *W* layer in $LuFe_2O_4$ crystal. The red and blue circles represent Fe^{3+} and Fe^{2+}, respectively, and the yellow arrow indicates the direction of polarization. (b) Schematic diagram showing how *W* layers are stacked along the *c*-axis direction in a $LuFe_2O_4$ crystal. The gray block indicates a stack of several *W* layers with aligned polarization directions, and the thickness (correlation length) is estimated to be approximately 50 nm [10]. (c) Azimuth angle dependence of *a*-axis polarized (red circle) and *b*-axis polarized SHG (red circle) in the *ab* plane. (d) Azimuth angle dependence of *a*-axis polarized (red circle) and *c*-axis polarized SHG (red circle) in the *ac* plane. The solid lines are the fitting result assuming monoclinic *Cm*.

$\boldsymbol{P}^{(2)}$ represents the second-order nonlinear polarization. Our recent studies reported observations of SHG and its azimuth angle dependence in a single crystal [20] and thin film [21] of $YbFe_2O_4$, clarifying not only that the crystal has a polar structure but that the symmetry belongs to point group *Cm* of the monoclinic crystal. Figure 1(c) shows the azimuth angle dependence of I_{SH} on the *ab* plane of the $LuFe_2O_4$ crystal used in this study. Red circles represent I_{SH} polarized in the *a*-axis direction (I^a_{ab}) and blue circles in the *b*-axis direction (I^b_{ab}). The polarization of an incident electric field was rotated using a half-wave plate to the azimuth angle θ, which is defined as the angle between the polarization of the incident electric field and the *a* axis. For both polarizations, a four-leaf cloverlike azimuth angle dependence was observed, similar to $YbFe_2O_4$. Under the *Cm* point group symmetry, the reduced $\chi^{(2)}$ tensor is represented as follows [22].

$$\chi^{(2)} = \begin{pmatrix} d_{11} & d_{12} & d_{13} & 0 & d_{15} & 0 \\ 0 & 0 & 0 & d_{24} & 0 & d_{26} \\ d_{31} & d_{32} & d_{33} & 0 & d_{35} & 0 \end{pmatrix}. \quad (1)$$

Using this, when light is irradiated on the *ab* plane, the azimuth angle dependence of the I_{SH} radiated in the *a*-axis and *b*-axis polarization is described as

$$I^a_{ab} \propto (d_{11}\cos^2\theta + d_{12}\sin^2\theta)^2, \quad (2)$$

$$I^b_{ab} \propto (d_{26}\sin^2\theta)^2. \quad (3)$$

The solid lines in Fig. 1(c) represent the fitting results of the observed I_{ab} using Eqs. (2) and (3), indicating that the $LuFe_2O_4$ crystal also has the symmetry belonging to point group *Cm*. On the basis of those results of SHG, in this study, we investigate the ferroelectric polarization dynamics and its anisotropy in $LuFe_2O_4$ through the time-resolved SHG measurements after optically disturbing the alignment of Fe ions and reveal not only a hidden photoexcited state created by light but try to photonically control the electronic ferroelectricity on a femtosecond scale at room temperature.

II. EXPERIMENT

The $LuFe_2O_4$ single crystals were synthesized using the floating zone method: Fe_2O_3 and Lu_2O_3 powders were mixed in a prescribed ratio, shaped under hydrostatic pressure, and sintered in air for 10 h. The sintered rod was then melted by a floating zone furnace to obtain a single crystal [10,23]. Details about evaluating the crystallinity and the development of charge order of a synthesized crystal was performed in Supplemental Material 2 [24]. The crystal orientation was determined using x-ray diffraction measurement, and the *ab* and *ac* planes were obtained by cutting with a diamond cutter. The *a* and *c* axes polarized reflectivity spectra were measured using a Fourier transform interferometer and a grating spectrometer. Optical conductivity spectra were derived from reflectivity based on Kramers-Kronig analysis. Time-resolved SHG measurement was conducted with a regenerated amplified mode-locked Ti:sapphire laser (wavelength ≈800 nm, pulse with ≈30 fs, repetition rate: 1 kHz) as a light source. [The experimental setup is shown in Fig. 2(a).] The laser pulse was split into two pulses; one of them is used for the pump light and directly irradiating the sample to resonant from *d*-*d* transitions in $LuFe_2O_4$. An optical parametric amplifier was used to transfer the wavelength of another pulse into 1300 nm for probe light. The polarization direction of the pump light was always set parallel to the *a* axis, matching the polarization component of $LuFe_2O_4$. The polarization of the probe light (≈1300 nm) was controlled using a λ/2 plate before irradiating the sample. The incident angle of the probe light is estimated as about 10°. The emitted SHG light (650 nm) from the sample polarized in a specific direction was detected by a photomultiplier tube after removing the fundamental wave of 1300 nm with a high-pass filter and a grating spectrometer.

III. RESULTS AND DISCUSSIONS

To clarify the electronic structure of $LuFe_2O_4$ and its anisotropy, in Fig. 2(b), we show $\sigma(\omega)$ in $LuFe_2O_4$ polarized along the *a* axis (red line) and the *c* axis (blue line). In both polarization directions, there is a broad absorption peak at about 1.5 eV and a steep rise in absorption from around 3

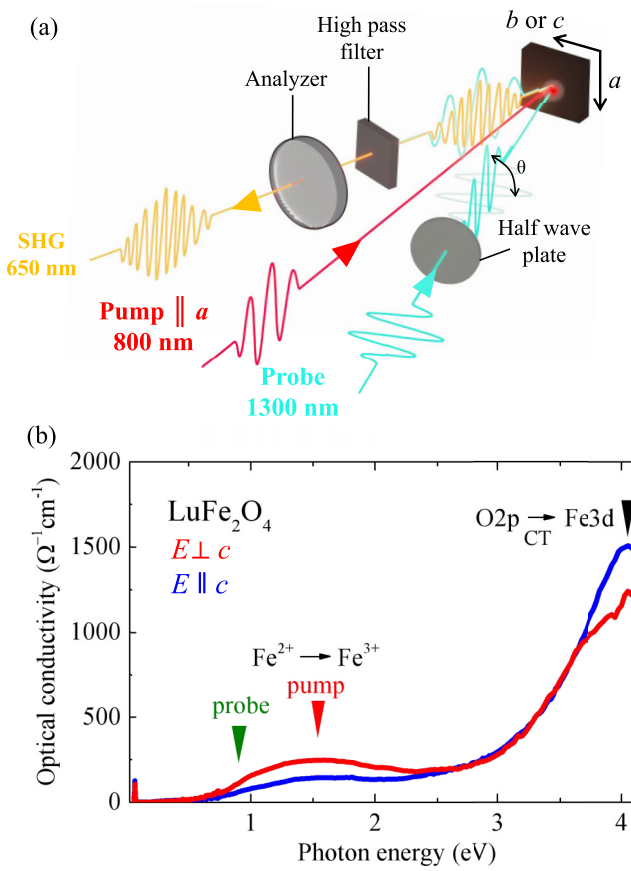

FIG. 2. (a) Schematic diagram of the experimental setup for measuring time-resolved SHG changes. (b) Optical conductivity spectra in $LuFe_2O_4$ crystal. The red line is the spectrum of $E \perp c$, and the blue line is the spectrum of $E||c$.

eV. According to previous literatures [25,26], the former is assigned to the $Fe^{2+} \rightarrow Fe^{3+}$ d-d transition and the latter to the O $2p \rightarrow$ Fe $3d$ charge-transfer transition. In this d-d transition, the spectral weight in the a-axis polarized $\sigma(\omega)$ is higher than that in the c-axis polarization. In $LuFe_2O_4$, the distance between Fe ions in the ab plane is ≈0.346 nm, which is shorter than the interplane distance, ≈0.416 nm [27,28]. This may be the reason for the difference in oscillator strength between the a-axis and c-axis polarized $\sigma(\omega)$. The downward red arrow in Fig. 2(b) indicates the energy of the excitation light used for the time-resolved SHG measurements. By the excitation causing the d-d transition, we can expect perturbing of the charge ordering of the threefold periodic Fe ions in the W-layer shown in Fig. 1(a), which realizes the electric polarization of $LuFe_2O_4$.

Figure 3(a) shows the time and excitation intensity dependence of the relative change in the intensity of the a-axis polarization component of the SHG light ($\Delta I^a_{ab}/I^a_{ab}$) after photoirradiation. Since the a-axis polarized pulse ($\theta = 0°$) is used as the probe light, the SHG observed here is due to the d_{11} component of Eq. (2). The time profile of $\Delta I^a_{ab}/I^a_{ab}$ shows a steep decrease immediately after light irradiation, then recovers slightly, but even after 200 ps I^a_{ab} hardly returns to the value before photoexcitation. The magnitude of this change increases as the excitation light density is increased, and a

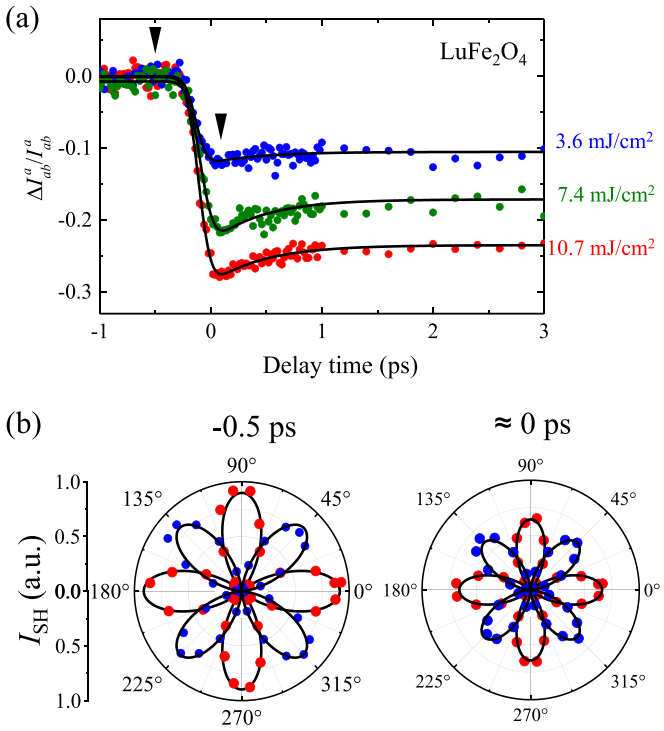

FIG. 3. (a) Time evolutions of a-axis polarized SHG intensity after photoexcitation of selected fluence on the ab plane of $LuFe_2O_4$ crystal. The solid line is the fitting result based on Eq. (4) (see text). (b) Azimuth angle dependence of SHG of the a-axis (red circle) and b-axis (blue circle) polarization before and immediately after photoexcitation.

decrease in SHG of ≈29% was observed at an excitation fluence of ≈10.7 mJ/cm^2 [29].

Figure 3(b) shows the azimuth angle dependence of I_{SH} emitted in a- and b-axis polarization before (−0.5 ps) and immediately after (≈0 ps) photoexcitation. (The excitation intensity is ≈10.7 mJ/cm^2.) Just after photoexcitation, the cloverlike angular profile shrank overall with maintaining its shape. This indicates that the magnitude of the electric polarization is reduced by photoexcitation, but the symmetry of the system (Cm) is conserved. The solid lines in the figure are the result of fitting based on Eqs. (2) and (3). The tensor components d_{11}, d_{12}, and d_{26} are found to decrease by ≈14% without changing their ratios compared to before excitation. It can be concluded that the charge ordering of Fe ions is disturbed by photoexcitation, resulting in a decrease in the ab-plane projection component of the electric polarization.

To quantitatively understand the time profile of $\Delta I^a_{ab}/I^a_{ab}$ in Fig. 3(a), we assume the following function when $t > 0$ as

$$F_{ab}(t) = A_0 - A_1 \exp\left(-\frac{t}{\tau_1}\right) - A_2 \exp\left(-\frac{t}{\tau_2}\right). \quad (4)$$

Here, τ_1 and τ_2 are decay times and A_0, A_1, and A_2 are constants to describe the time dependence. As shown by the solid lines in Fig. 3(a), we could well fit the observed time dependence by using Eq. (4) convoluted with the instrumental response function. The fitting result indicated that $\tau_1 \approx 0.12$ ps and $\tau_2 \approx 0.29$ ps at all excitation intensities.

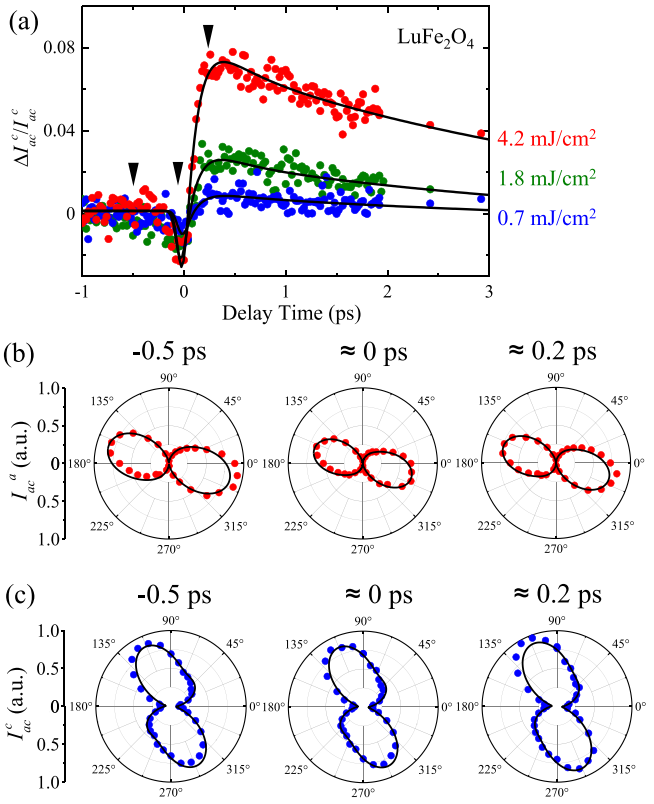

FIG. 4. (a) Time evolutions of *c*-axis polarized SHG intensity after photoexcitation of selected fluence on the *ac* plane of $LuFe_2O_4$ crystal. The solid line is the fitting result based on Eq. (5) (see text). (b) and (c) Azimuth angle dependence of *a*-axis (b) and *c*-axis (c) polarized SHG at −0.5, 0, and 0.2 ps.

The next issue to discuss is the photoinduced dynamics exhibited by the *c*-axis polarization component of SHG. Figure 1(d) shows the azimuth angle dependence of I_{SH} polarized along the *a* axis (red circles) and the *c* axis (blue circles) in the *ac* plane of the $LuFe_2O_4$ crystal in the ground state; unlike the case for the *ab* plane, a distorted angular profile is observed. Since this asymmetric profile could not be described by only a single domain with *Cm* symmetry, we postulated the existence of domains in which only the projection component of the polarization onto the *ab* plane is inverted (60° domain), as shown in Supplemental Material 1 [24]. This is caused by a 180° rotation of the phase of the *W*-layer stacking and is often observed in this system [30]. The angular profile of the SHG observed in the *ac* plane is given by Eqs. (S1) and (S2) in Supplemental Material 1 [24]. The SHG signal generated in this case is described by d_{11} plus other tensor components (d_{13}, d_{15}, d_{31}, d_{33}, and d_{35}). The solid line in Fig. 1(d) is the result of fitting using Eqs. (S1) and (S2), confirming that the symmetry of the $LuFe_2O_4$ crystal can be described by *Cm*, even when measured on the *ac* plane.

Figure 4(a) shows the time dependence of the relative change in the *c*-axis polarized SHG pulse ($\Delta I^c_{ac}/I^c_{ac}$) after photoexcitation in the *ac* plane of the $LuFe_2O_4$ crystal. (The polarization angle of the incident probe light is $\theta = 110°$, the direction in which the *c*-axis polarization component of the generated SHG light is strongest.) Immediately after photoexcitation, $\Delta I^c_{ac}/I^c_{ac}$ decreases instantaneously as in the *ab* plane case [Fig. 3(a)], but then it is observed to increase after ≈0.2 ps. Furthermore, increased I_{SH} slowly returns to the preexcitation state. This result is qualitatively different from the dynamics seen in the time profile of $\Delta I^a_{ab}/I^a_{ab}$ in Fig. 3(a), where suppression of the SHG survives long after photoexcitation, and indicates that the *c*-axis polarization component increases after photoexcitation and slowly returns to the original state. Such anisotropic polarization dynamics is a characteristic feature of $LuFe_2O_4$ crystal.

To further quantify the dynamics in the *ac* plane, we assume the following function $F_{ac}(t)$ when $t > 0$ to reproduce the time evolution of the SHG after photoexcitation:

$$F_{ac}(t) = B_0 - B_1 \exp\left(-\frac{t}{\tau_1}\right) - B_2 \exp\left(-\frac{t}{\tau_2}\right) - B_3 \exp\left(-\frac{t}{\tau_3}\right). \quad (5)$$

Here, τ_1 and τ_2 are the relaxation times and τ_3, B_0, B_1, B_2, and B_3 are fitting parameters to describe each amplitude. We performed the fitting analysis by convoluting the SHG time profiles with the instrumental response function, as we did in the *ab* plane. As a result, good fits were obtained for all excitation fluences as represented by the solid line in Fig. 4(a). The magnitude of τ_3 is almost the same for all excitation densities and can be estimated as $\tau_3 \approx 4.5$ ps.

The unique behavior of the SHG dynamics in the *ac* plane indicates that variations in tensor components other than d_{11} and d_{12} also play an important role in the polarization dynamics of the system. Figures 4(b) and 4(c) show the azimuth angle dependence of the SHG polarized along the *a* axis (b) and the *c* axis (c), which were measured before, just after, and 0.2 ps after the photoirradiation. [The filled triangles in Fig. 4(a) denote the respective delay times.] At all delay times, the azimuth angle dependence of SHG retains the asymmetric shape seen before photoexcitation. However, the magnitude of the overall angular profile decreases immediately after optical excitation and then increases again after 0.2 ps. We performed a fitting analysis of this azimuth angle dependence in the *ac* plane based on Eqs. (S1) and (S2) and calculated the $\chi^{(2)}$ tensor components at each delay time. The solid black lines in Figs. 4(b) and 4(c) show the results of the fitting analysis. Figure 5 shows the time dependence of the relative rates of change of d_{11}, d_{35}, and d_{33} obtained from the fitting analysis. It shows that d_{11} and d_{35} decrease immediately after excitation and then recover slightly but remain negative in sign, whereas d_{33} slightly decreases immediately after irradiation and then increases by ≈ 3% more than before photoexcitation. Since d_{11} and d_{33} are proportional to the degree of inversion symmetry breaking in the *a*- and *c*-axis directions, respectively, it can be seen that at ≈ 0.2 ps after photoexcitation, the in-plane component of polarization is reduced, but the *c*-axis component of polarization is rather enhanced compared to before the excitation.

Based on these results, we discuss the polarization dynamics of $LuFe_2O_4$. Figure 6 shows a schematic diagram of the change of state of the *W*-layer and the Fe ions in it upon photoexcitation. The in-plane *d*-*d* transition of $Fe^{2+} \rightarrow Fe^{3+}$

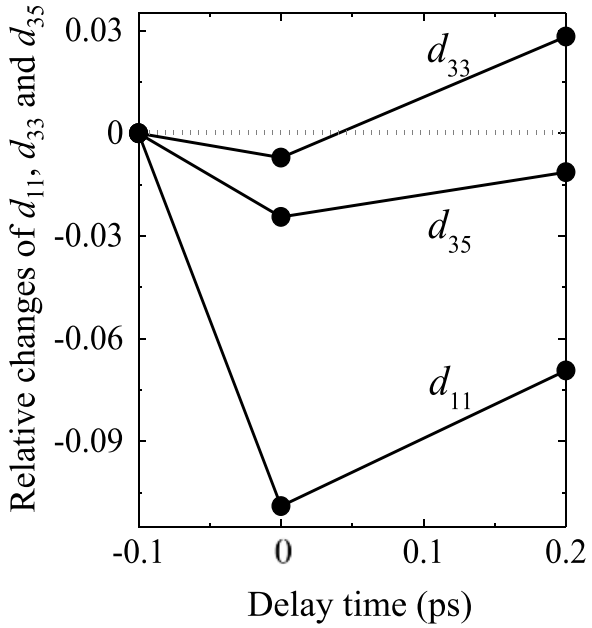

FIG. 5. Time evolution of the selected reduced $\chi^{(2)}$ tensor components (d_{11}, d_{35}, d_{33}) after photoexcitation.

by photoexcitation leads to the Frank-Condon (FC) state in which the threefold periodic order of Fe^{2+} and Fe^{3+} in the ground state is disturbed [see Fig. 1(a)]. Via the FC state, a photoexcited state appears: First, the in-plane SHG signal of $LuFe_2O_4$ decreases significantly with the time constant of τ_1 (≈ 0.12 ps), while not in the interplane I_{SH}, indicating that the W-layer is composed of a Fe^{2+}-rich layer (indicated by thin red circles) and a Fe^{3+}-rich layer (indicated by thin blue circles) whose threefold periodic order remains disturbed. In this state, the direction of polarization is on average oriented toward the c-axis, which explains that d_{11} decreases but d_{33} scarcely changes. The right panel of Fig. 6(b) shows a schematic of the correlation of the c-axis polarization described in Fig. 1(b). In this time region, the gray blocks are composed of the charge disproportionated W-layers and stacked in the c-axis direction, keeping the correlation length seen in the ground state ($\approx$50 nm).

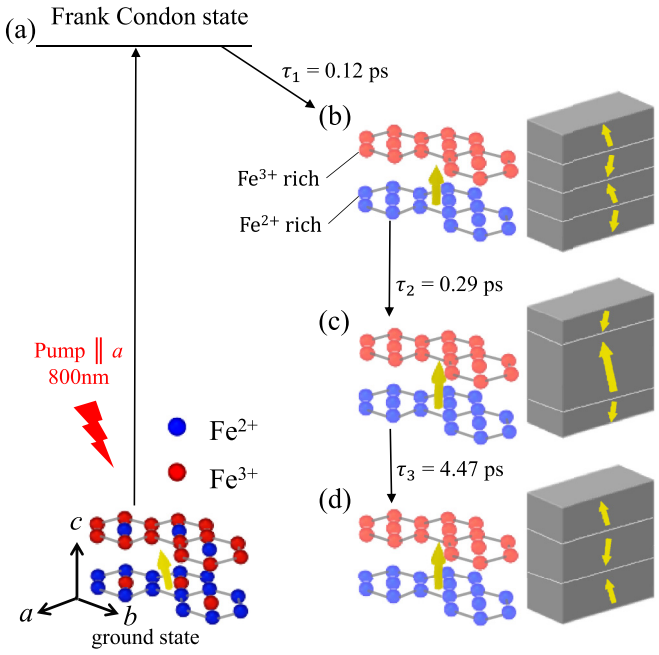

FIG. 6. Schematic diagram of the dynamics of iron ions in the W-layer after photoexcitation in $LuFe_2O_4$. By irradiating the crystal with 800 nm pulse, the ground state with the threefold periodic order of Fe^{2+} and Fe^{3+} is disturbed and a Franck-Condon state occurs (a). After that, the W-layer becomes composed of an average Fe^{2+}-rich layer (light red) and an Fe^{3+}-rich layer (light blue) and stacking of W-layers successively varies (b)–(d). The gray block in the right column represents the W-layer stacking described in Fig. 1(b). The yellow arrow indicates the polarization direction.

What should be noted is the dynamics represented by the time constant τ_2 (≈ 0.29 ps) [Fig. 6(c)]. In this time region, the I_{SH} in the ab plane slightly rises due to the relaxation of some small region of the excited area [18], but most of the photoexcited region remains reduced and the W-layers still lose their in-plane threefold periodic order as shown in Fig. 6(b). By contrast, the interplane SHG shows an instantaneous increase. The reason for this is not yet clear, but one possibility is that the correlation length of the electric polarization has increased as shown in the right schematics of Fig. 6(c). In the c-axis polarized SHG radiation, if the volume of one polarization domain increases, the total I_{SH} also increases because of the reduction of interference. In the present situation, the W-layers are composed of Fe^{2+}-rich and Fe^{3+}-rich layers without in-plane long-range order, and it is possible that the total electric polarization direction is more aligned along the c axis to gain long-range Coulomb energy between the W-layers and that the correlation length along the c axis increases. According to this scenario, the variation of d_{33} in Fig. 5 results from the reorientation of the stack of the Fe^{2+}-rich and Fe^{3+}-rich layers, suggesting that the c-axis correlation increases by about 3% at 0.2 ps.

This increased SHG slowly recovers with a time constant of τ_3 ($\approx$4.5 ps), and the correlation length of the c-axis polarization returns to the original state [Fig. 6(d), right]. Thus, not only the charge ordering state of the Fe ions but also the changes in the c-axis correlation between W layers are intertwined and determine the ultrafast anisotropic polarization dynamics of $LuFe_2O_4$.

Another possible scenario for the origin of the observed instantaneous increase in the c-axis polarized SHG in $LuFe_2O_4$ is a change of the crystal structure itself with photoexcitation. In the previous section, we considered a scenario in which the crystal hardly changes and the ordered state of Fe ions varies. However, if the position of the ions constituting the crystal moves upon photoexcitation, the magnitude of the SHG as well as $\chi^{(2)}$ tensor components of the system changes as a result. For example, if the distance between the W-layers increases after light irradiation, the c-axis magnitude of the electric polarization shown in Fig. 1(a) can increase, and the magnitude of the d_{33} component of the $\chi^{(2)}$ tensor should increase accordingly. To investigate this experimentally, in addition to first-principles calculations, time-resolved crystallographic studies on the 100-fs scale using femtosecond x-ray and electron beam pulses, which have been actively pursued

in recent years [13,31], are needed, and this would deserve future research.

IV. SUMMARY

Optical conductivity, SHG azimuth angle dependence, and anisotropy of femtosecond time-resolved pump-probe SHG changes were measured for $LuFe_2O_4$ single crystal which is noticed as an electronic ferroelectric material. The optical conductivity spectrum showed anisotropy consistent with charge order alignment. SHG azimuth angle dependence on the *ab* plane and the *ac* plane confirmed $LuFe_2O_4$ has monoclinic *Cm* symmetry and determined the ratio of the $\chi^{(2)}$ tensor components. Time-resolved SHG measurements revealed anisotropic dynamics: 800-nm pulse irradiation causing a $Fe^{2+} \rightarrow Fe^{3+}$ transition that disturbs iron ion charge order reduces I_{SH} emitted from the *ab* plane, whereas it increases I_{SH} emitted from the *ac* plane, indicating enhancement of the *c*-axis component of the electric polarization by light. These anisotropic dynamics were discussed in terms of charge order and disorder, and variations of the correlation length of polarization between *W* layers. This study demonstrates the ultrafast and room-temperature control of electric polarization induced by electronic order by light irradiation, suggesting possibilities for applications in high-speed optical communication and ferroelectric memory devices.

ACKNOWLEDGMENTS

The authors thank R. Seimiya, R. Ota, S. Ogasawara, K. Fujiwara, and T. Fujii for their technical assistance and discussion. This research was supported by Japan Society for the Promotion of Science (JSPS) KAKENHI Grants No. JP18H05208, No. JP18H02057, No. JP19H01827, No. JP22H01153, No. JP22H01942, No. JP22H01149, and No. JP20H05147.

[1] N. Ikeda, H. Ohsumi, K. Ohwada, K. Ishii, T. Inami, K. Kakurai, Y. Murakami, K. Yoshii, S. Mori, Y. Horibe, and H. Kito, Nature (London) **436**, 1136 (2005).

[2] P. Monceau, F. Ya. Nad, and S. Brazovskii, Phys Rev. Lett. **86**, 4080 (2001).

[3] K. Yamamoto, S. Iwai, S. Bokyo, A. Kashiwazaki, F. Hiramatsu, C. Okabe, N. Nishi, and K. Yakushi, J. Phys. Soc. Jpn. **77**, 074709 (2008).

[4] T. Portengen, Th. Ostreich, and L. J. Sham, Phys. Rev. B **54**, 17452 (1996).

[5] S. Konishi, D. Urushihara, T. Hayakawa, K. Fukuda, T. Asaka, K. Ishii, N. Naoda, M. Okada, H. Akamatsu, H. Hojo, M. Azuma, and K. Tanaka, Phys. Rev. B **108**, 014105 (2023).

[6] N. Ikeda, K. Kohn, N. Myouga, E. Takahashi, H. Kitoh, and S. Takekawa, J. Phys. Soc. Jpn. **69**, 1526 (2000).

[7] N. Ikeda, K. Kohn, H. Kito, J. Akimitsu, and K. Siratori, J. Phys. Soc. Jpn. **63**, 4556 (1994).

[8] T. Nagata, Y. Fukada, M. Kawai, J. Kano, T. Kambe, E. Dudzik, R. Feyerherm, P. E. Janolin, J. M. Kiat, and N. Ikeda, Ferroelectrics **442**, 45 (2013).

[9] S. Ishihara, J. Phys. Soc. Jpn. **79**, 011010 (2010).

[10] K. Fujiwara, T. Karasudani, K. Kakurai, W. T. Lee, K. C. Rule, A. J. Studer, and N. Ikeda, J. Phys. Soc. Jpn. **88**, 044701 (2019).

[11] H. L. Williamson, T. Mueller, M. Angst, and G. Balakrishnan, J. Cryst. Growth **475**, 44 (2017).

[12] *Photoinduced Phase Transitions*, edited by K. Nasu (World Scientific, Singapore, 2004).

[13] S. Koshihara, T. Ishikawa, Y. Okimoto, K. Onda, R. Fukaya, M. Hada, Y. Hayashi, S. Ishihara, and T. Luty, Phys. Rep. **942**, 1 (2022).

[14] T. Miyamoto, H. Yada, H. Yamakawa, and H. Okamoto, Nat. Commun. **4**, 2586 (2013).

[15] R. Mankowsky, A. von Hoegen, M. Först, and A. Cavalleri, Phys. Rev. Lett. **118**, 197601 (2017).

[16] Y. Okimoto, P. Xia, J. Itatani, H. Matsushima, T. Ishikawa, S. Koshihara, and S. Horiuchi, APL Mater. **10**, 090702 (2022).

[17] H. Itoh, K. Itoh, K. Anjyo, H. Nakaya, H. Akahama, D. Ohishi, S. Saito, T. Kambe, S. Ishihara, N. Ikeda, and S. Iwai, J. Lumin. **133**, 149 (2013).

[18] Y. Okimoto, S. Naruse, R. Fukaya, T. Ishikawa, S. Koshihara, K. Oka, M. Azuma, K. Tanaka, and H. Hirori, Phys. Rev. Appl. **7**, 064016 (2017).

[19] N. Sono, Y. Kinoshita, N. Kida, T. Itoh, H. Okamoto, and T. Miyamoto, J. Phys. Soc. Jpn. **90**, 033703 (2021).

[20] K. Fujiwara, Y. Fukada, Y. Okuda, R. Seimiya, N. Ikeda, K. Yokoyama, H. Yu, S. Koshihara, and Y. Okimoto, Sci. Rep. **11**, 4277 (2021).

[21] H. Yu, Y. Okimoto, A. Morita, S. Shimanuki, K. Takubo, T. Ishikawa, S. Koshihara, R. Minakami, H. Itoh, S. Iwai, N. Ikeda, T. Sakagami, M. Nozaki, and T. Fujii, Materials **16**, 1989 (2023).

[22] A. Authier, *International Tables for Crystallography D: Physical Properties of Crystals* (International Union of Crystallography, Chester, UK, 2013).

[23] K. Fujiwara, T. Karasudani, M. Fukunaga, H. Kobayashi, J. Kano, P-E. Janolin, J-M. Kiat, Y. Nogami, R. Kondo, and N. Ikeda, Ferroelectrics **512**, 85 (2017).

[24] See Supplemental Material at http://link.aps.org/supplemental/10.1103/PhysRevMaterials.8.064402 for crystal domains, crystallinity evaluation, and time-resolved reflectance measurements.

[25] X. S. Xu, M. Angst, T. V. Brinzari, R. P. Hermann, J. L. Musfeldt, A. D. Christianson, D. Mandrus, B. C. Sales, S. McGill, J.-W. Kim, and Z. Islam, Phys. Rev. Lett. **101**, 227602 (2008).

[26] R. C. Rai, A. Delmont, A. Sprow, B. Cai, and M. L. Nakarmi, Appl. Phys. Lett. **100**, 212904 (2012).

[27] H. J. Xiang and M.-H. Whangbo, Phys. Rev. Lett. **98**, 246403 (2007).

[28] J. Bourgeois, M. Hervieu, M. Poienar, A. M. Abakumov, E. Elkaim, M. T. Sougrati, F. Porcher, F. Damay, J. Rouquette, G. Van Tendeloo, A. Maignan, J. Haines, and C. Martin, Phys. Rev. B **85**, 064102 (2012).

[29] One might consider that the large variation of SHG is due to the change of reflectance of $LuFe_2O_4$ by the photoexcitation. In Supplemental Material 3 [24], we added the data of time-resolved relative change in reflectance ($\Delta R/R$) at 1300 nm after pumping of an 800-nm pulse in the *ab* and *ac* planes obtained

with the same pump pulse for the measurement of $\Delta I^a_{ab}/I^a_{ab}$. As seen in the Supplemental Material figures, the value of $\Delta R/R$ at 1300 nm is less than 3% (0.5% in the *ac* plane), and even smaller compared to those of SHG. This result strongly indicates that the reflectance change alone cannot account for the large change of SHG.

[30] T. Sakagami, R. Ota, J. Kano, N. Ikeda, and T. Fujii, CrystEngComm **23**, 6163 (2021).

[31] K. Takubo, S. Banu, S. Jin, M. Kaneko, W. Yajima, M. Kuwahara, Y. Hayashi, T. Ishikawa, Y. Okimoto, M. Hada, and S. Koshihara, Rev. Sci. Instrum. **93**, 053005 (2022).